

Corrosion of Ti_3SiC_2 in an Ar-1% SO_2 atmosphere between 800 and 1100 °C

Thuan Dinh Nguyen^a, Sang-Whan Park^b and Dong-Bok Lee^{a,*}

^aSchool of Advanced Materials Science and Engineering, Sungkyunkwan University, Suwon 440-746, Korea

^bMaterials Science and Technology Research Division, KIST, Seoul 136-791, Korea

Ti_3SiC_2 compounds were synthesized by a powder metallurgical route, and corrosion-tested at 800, 900, 1000 and 1100 °C for up to 50 h under an Ar-1% SO_2 gas atmosphere. The scale formed consisted primarily of an outer rutile- TiO_2 layer and an inner (rutile- TiO_2 + amorphous SiO_2)-mixed layer. Sulfur was mainly enriched at the scale-matrix interface. The corrosion progressed mainly via oxidation rather than sulfidation. Ti_3SiC_2 displayed excellent corrosion resistance due mainly to its high Si content that formed a SiO_2 barrier layer.

Key words: Ti_3SiC_2 , Corrosion, Oxidation, Sulfidation.

Introduction

The ternary carbide, Ti_3SiC_2 , is a remarkable material for a myriad of applications, because of its unique combination of metallic and ceramic properties [1]. Like metals, it has excellent electrical and thermal conductivities, high toughness, a high fatigue-crack growth threshold, low hardness, good machinability, and a high-thermal shock resistance. Like ceramics, it displays excellent chemical resistance, a high Young's modulus, and high temperature strength. In order to utilize Ti_3SiC_2 in high-temperature structural components, the oxidation of Ti_3SiC_2 -base materials was studied. Good oxidation resistance was obtained up to 1100 °C in air [1-6]. Hot corrosion tests in the mixtures of Na_2SO_4 - NaCl [7] and LiCO_3 - K_2CO_3 [8] indicated that Ti_3SiC_2 was prone to hot corrosion attack. In this study, the corrosion performance of Ti_3SiC_2 under an (Ar + 1% SO_2) atmosphere was investigated between 800 and 1100 °C, because resistance to sulfur-containing atmospheres is vital in petrochemical plants, coal-gasification units, turbines, heat exchangers, etc. Such a study has not yet been performed as far as we know. The characteristics of the scales formed and the corrosion resistance and mechanism for Ti_3SiC_2 were investigated.

Experimental

Powders of TiC_x ($x < 44 \mu\text{m}$, $x = 0.6$) and Si ($< 70 \mu\text{m}$, 99.7% purity) were weighed in a molar ratio of 3 to 1, mixed in a shaker mill for 10 minutes, and hot pressed at 1360 °C under a pressure of 25 MPa for 90 minutes in flowing Ar gas to fabricate bulk Ti_3SiC_2 with dimensions of $19 \text{ mm} \phi \times$

10 mm. The synthesized samples were cut into small coupons with dimensions of $10 \times 5 \times 5 \text{ mm}^3$, polished with a 1000 grit emery paper, and ultrasonically cleaned in acetone and methanol for corrosion tests at 800, 900, 1000, and 1100 °C for up to 50 h in a commercial-grade Ar (99.999% purity)-1% SO_2 (99.9% purity) gas mixture. The corroded samples were investigated by means of a scanning electron microscope (SEM) equipped with an energy dispersive X-ray spectrometer (EDS), an electron probe microanalyzer (EPMA), and an X-ray diffractometer (XRD).

Results and Discussion

Figs. 1(a) and (b) show the SEM image and the corresponding XRD pattern of Ti_3SiC_2 . Fully dense

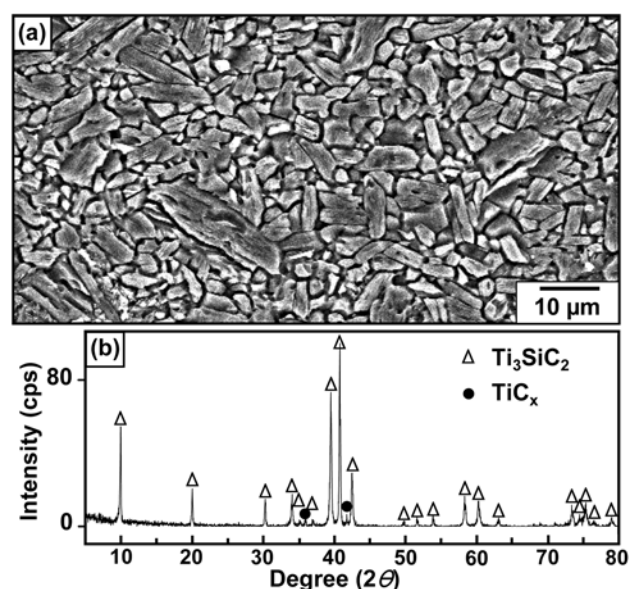


Fig. 1. Etched SEM microstructure (a), and XRD pattern (b) of Ti_3SiC_2 synthesized.

*Corresponding author:
 Tel : +82-31-290-7355
 Fax: +82-31-290-7379
 E-mail: dlee@skku.ac.kr

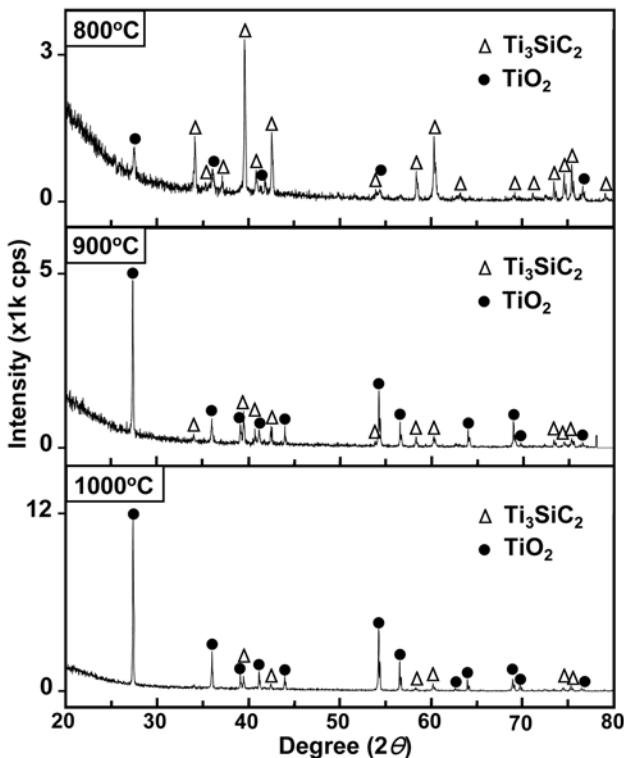


Fig. 2. XRD patterns of Ti_3SiC_2 after corrosion for 20 h between 800 and 1000 °C in Ar-1% SO_2 .

specimens were obtained (Fig. 1(a)). The measured density was 4.518 g/cm^3 , with a relative density of more than 99.5% of the theoretical value. The lamellar grains had dimensions of $16 \mu\text{m}$ in length and $4 \mu\text{m}$ in thickness. In addition to the Ti_3SiC_2 matrix, a small amount of residual TiC_x was also present as an impurity (Fig. 1(b)). TiC is a common impurity in Ti_3SiC_2 [1-5], and decreases the oxidation resistance of Ti_3SiC_2 [1, 3].

Fig. 2 shows the XRD patterns of Ti_3SiC_2 after corrosion for 20 h at 800, 900 and 1000 °C. For all of the test temperatures, rutile- TiO_2 was the only corrosion product. With an increase in temperature, TiO_2 peaks became stronger while Ti_3SiC_2 peaks became weaker owing to the thickening of the scale. Even after corrosion at 1000 °C for 20 h, Ti_3SiC_2 peaks were still noticeable, indicating that the matrix had superior corrosion resistance. On the other hand, it is known that Ti_3SiC_2 oxidizes to rutile- TiO_2 and amorphous SiO_2 , accompanying the evolution of CO or CO_2 gases [1, 2, 4]. Under the current Ar-1% SO_2 gas atmosphere, no sulfides were detected by XRD, indicating that the oxidizing tendency was stronger than the sulfidizing tendency. Silicon seemed to oxidize to amorphous SiO_2 in this study. It is noted that the semi-protective TiO_2 grew much faster than the extremely protective SiO_2 . Hence, the superior corrosion resistance of Ti_3SiC_2 originated from Si.

Fig. 3 shows a SEM image of Ti_3SiC_2 after corrosion at 800 °C for 50 h. A dense, uniform oxide scale of about $1.6 \mu\text{m}$ -thickness was formed. Here, sulfides were hardly detected, because the oxides were the more stable.

Fig. 4 shows the SEM/EDS analytical result of Ti_3SiC_2

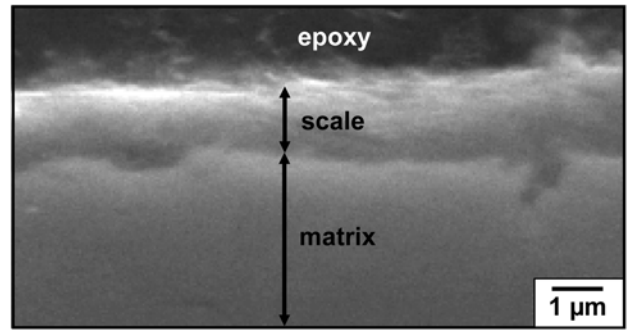


Fig. 3. SEM cross sectional image of Ti_3SiC_2 after corrosion at 800 °C for 50 h in Ar-1% SO_2 .

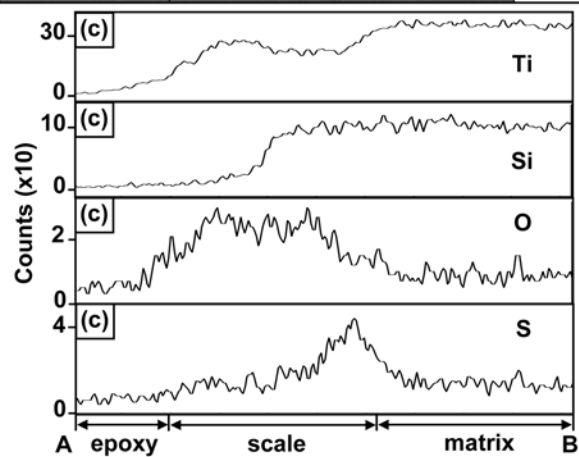
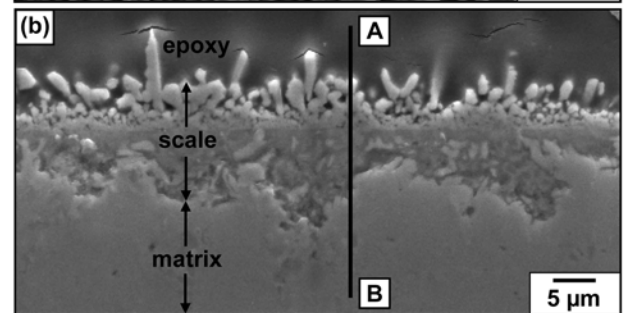
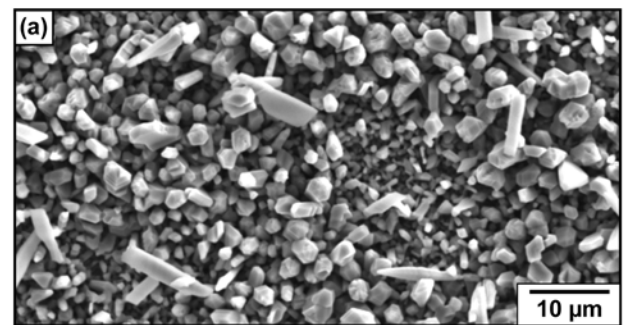


Fig. 4. SEM/EDS analyses on the Ti_3SiC_2 after corrosion at 900 °C for 50 h in Ar-1% SO_2 . (a) top view, (b) cross sectional image, (c) EDS line profiles along A-B.

after corrosion at 900 °C for 50 h. As the corrosion progressed, rutile having a high growth rate soon overgrew silica, covered the entire surface and progressively grew to produce coarse oxide grains. Rutile- TiO_2 grains formed on

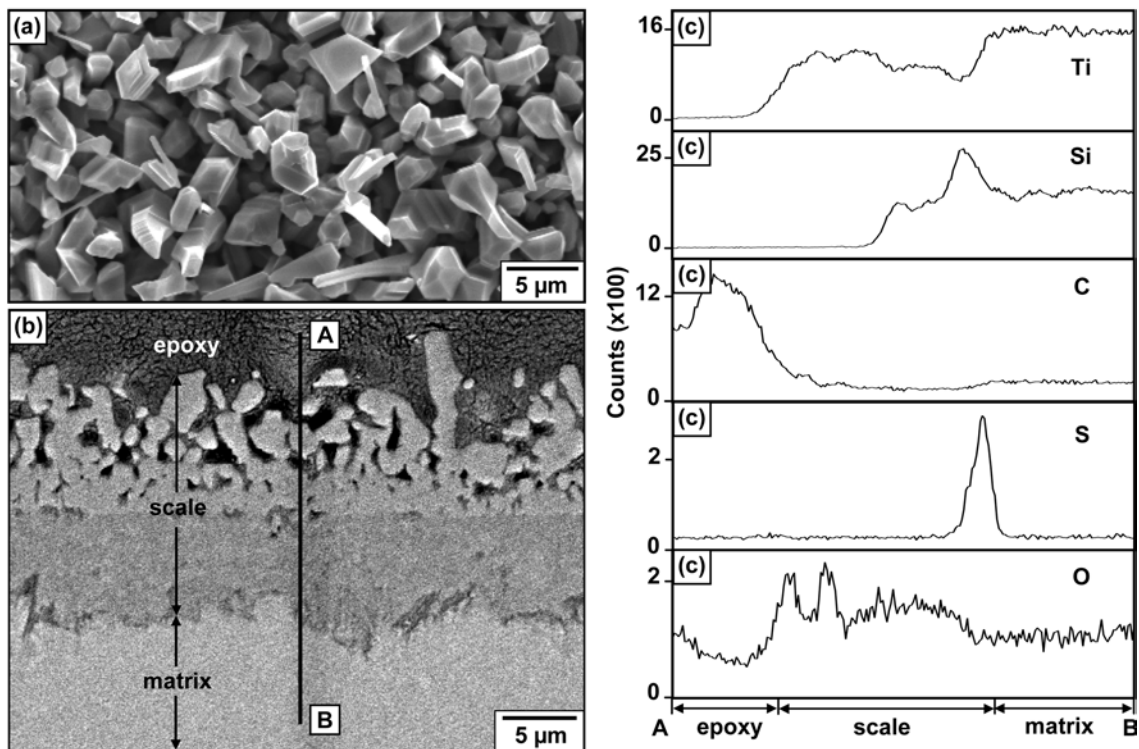


Fig. 5. EPMA analyses on the Ti_3SiC_2 after corrosion at 1000 °C for 50 h in Ar-1% SO_2 . (a) top view, (b) backscattered electron (BSE) image of the cross section, (c) line profiles along A-B.

the surface (Fig. 4(a)). Figs. 4(b) and (c) indicate that the scale consisted primarily of an outer TiO_2 layer, and an inner ($\text{TiO}_2 + \text{SiO}_2$)-mixed layer. Such a scale structure was also found in the oxide scale under an oxidizing atmosphere [1-6]. Sulfur was present around the scale/matrix interface (Fig. 4(c)). Generally, sulfides are undesirable, because of their fast growth rate. The absence of sulfides in Fig. 2 may indicate that the amount of sulfides formed was small.

Fig. 5 shows the EPMA analytical result of Ti_3SiC_2 after corrosion at 1000 °C for 50 h. The surface scale grew to a characteristic coarse, pillar-like rutile- TiO_2 (Fig. 5(a)). The oxide scale was divided into the outer TiO_2 layer, and the inner ($\text{TiO}_2 + \text{SiO}_2$)-mixed layer. Sulfur was weakly segregated at the scale-matrix interface. Carbon had escaped from the scale into the air. Despite sulfur inside the scale, Ti_3SiC_2 was highly resistant to sulfidation due mainly to the formation of the protective SiO_2 , which acted as a diffusion barrier. It is worthwhile noting that the very low expansion coefficient and fracture toughness of SiO_2 generally make the scales susceptible to failure. Also, voids, which form in the scale, act as stress concentrators, provide channels for oxygen and sulfur diffusion, and adversely affect the scale integrity or adherence. Moreover, the oxidation of Ti_3SiC_2 to TiO_2 and SiO_2 results in 194% volume expansion. However, the scales formed on Ti_3SiC_2 was generally adherent and crack-free [1, 4]. Stresses developed in the scale during corrosion were relieved effectively, despite the severe

corrosion condition imposed on the sample shown in Fig. 5.

Fig. 6 shows the EPMA analytical result of Ti_3SiC_2 after corrosion at 1100 °C for 20 h. As was shown in Figs. 4 and 5, the corrosion of Ti_3SiC_2 resulted in the formation of an outer TiO_2 layer and an inner ($\text{TiO}_2 + \text{SiO}_2$)-mixed layer. Sulfur was strongly segregated at the scale-matrix interface. Carbon was nearly absent in the scale. To understand the corrosion mechanism, a marker test was performed by spraying fine Pt particles on the matrix surface prior to corrosion. Pt particles were located at the bottom of the outer TiO_2 layer, indicating that the outer TiO_2 scale grew by the outward diffusion of Ti ions, while the growth of the inner scale was due to the inwardly diffusing oxygen and sulfur ions. It is noted that TiO_2 grows primarily by either the outward diffusion of interstitial Ti^{+4} ions or the inward diffusion of O^{2-} ions [9], and the growth of SiO_2 is dominated by the inward diffusion of oxygen [10].

Conclusions

During corrosion of Ti_3SiC_2 , Ti diffused outwards to form the outer TiO_2 layer, and oxygen transported inwards to form the inner ($\text{TiO}_2 + \text{SiO}_2$)-mixed layer. At the same time, the carbon in the Ti_3SiC_2 escaped into the air, whereas sulfur diffused inwards to form sulfides at the scale-matrix interface. No sulphides were detected by XRD, owing to their small amount. The corrosion was dominated by oxidation rather than sulfidation. The slow-growing SiO_2 provided the necessary corrosion resistance.

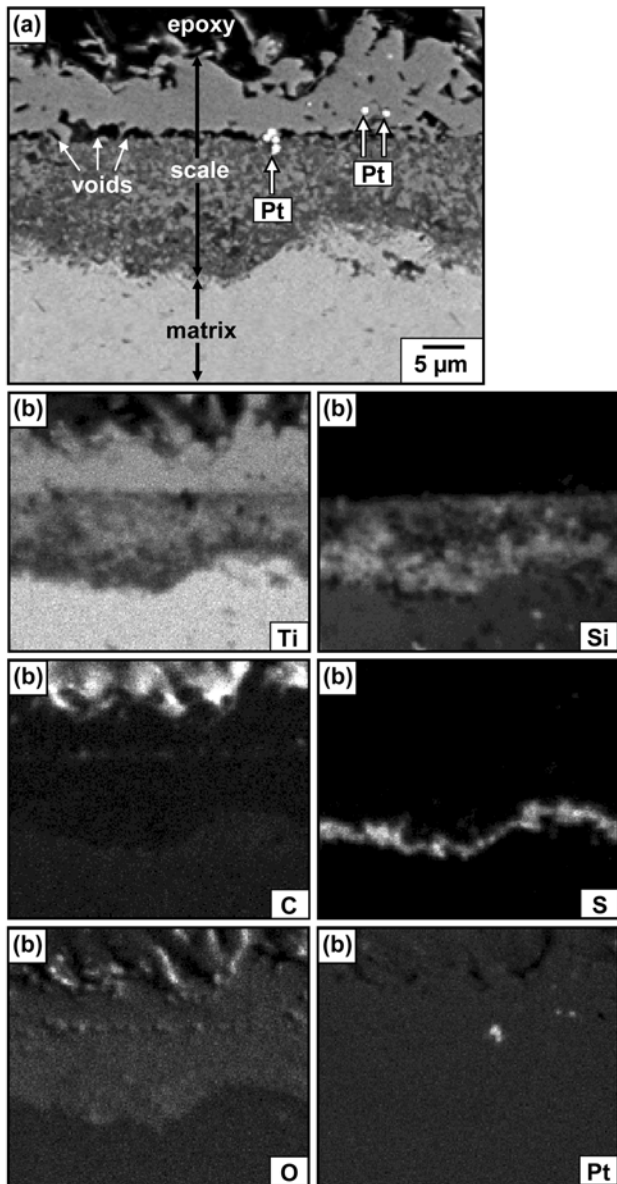


Fig. 6. EPMA analyses on the Ti_3SiC_2 after corrosion at 1100 °C for 20 h in Ar-1% SO_2 . (a) back-scattered electron (BSE) image of cross section, (b) elemental maps of some of the region shown in (a).

Acknowledgement

This work was supported by KICOS and MEST through the Korea-Ukraine Joint Research Program, Korea.

References

1. M.W. Barsoum, T. El-Raghy and L.U.J.T. Ogbuji, *J. Electrochem. Soc.* 144 (1997) 2508-2516.
2. N.F. Gao, Y. Miyamoto and D. Zhang, *J. Mater. Sci.* 34 (1999) 4385-4392.
3. Z. Sun, Y. Zhou and M. Li, *Acta Mater.* 49 (2001) 4347-4353.
4. Z. Sun, Y. Zhou and M. Li, *Oxid. Met.* 57 (2002) 379-394.
5. S.B. Li, L.F. Cheng and L.T. Zhang, *Mater. Sci. Eng. A* 341 (2003) 112-120.
6. T.D. Nguyen, J.H. Choi, S.W. Park and D.B. Lee, *J. Ceram. Proc. Res.* 8 (2007) 397-401.
7. G.M. Liu, M.S. Li, Y.C. Zhou and Y.M. Zhang, *J. Eur. Ceram. Soc.* 25 (2005) 1033-1039.
8. G.M. Liu, M.S. Li, Y.C. Zhou and Y.M. Zhang, *J. Eur. Ceram. Soc.* 23 (2003) 1957-1962.
9. Y.M. Chiang, D.P. Birnie III and W.D. Kingery, in "Physical Ceramics" (John Wiley & Sons, Inc, 1996) p. 109.
10. P. Kofstad, *Oxid. Met.* 44 (1995) 3-27.